Accepted Manuscript

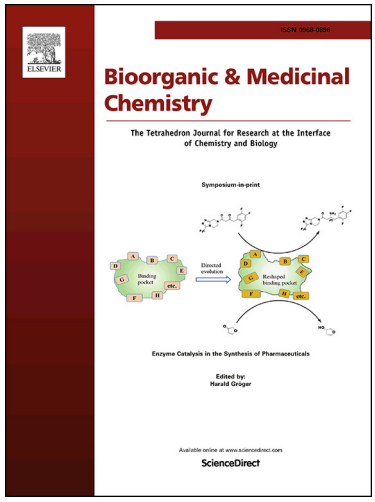

Synthesis, Structure-Activity Relationship and Molecular Docking Studies of 3-*O*-Flavonol Glycosides as Cholinesterase Inhibitors

Ehsan Ullah Mughal, Asif Javid, Amina Sadiq, Shahzad Murtaza, Muhammad Naveed Zafar, Bilal Ahmad Khan, Sajjad Hussain Sumra, Muhammad Nawaz Tahir, Kanwal, Khalid Mohammed Khan

PII: S0968-0896(18)30964-7
DOI: https://doi.org/10.1016/j.bmc.2018.05.050
Reference: BMC 14392

To appear in: *Bioorganic & Medicinal Chemistry*

Received Date: 22 May 2018
Revised Date: 30 May 2018
Accepted Date: 31 May 2018

Please cite this article as: Mughal, E.U., Javid, A., Sadiq, A., Murtaza, S., Zafar, M.N., Khan, B.A., Sumra, S.H., Nawaz Tahir, M., Kanwal, Khan, K.M., Synthesis, Structure-Activity Relationship and Molecular Docking Studies of 3-*O*-Flavonol Glycosides as Cholinesterase Inhibitors, *Bioorganic & Medicinal Chemistry* (2018), doi: https://doi.org/10.1016/j.bmc.2018.05.050

Synthesis, Structure-Activity Relationship and Molecular Docking Studies of 3-*O*-Flavonol Glycosides as Cholinesterase Inhibitors

Ehsan Ullah Mughal[*a], Asif Javid[a], Amina Sadiq[b], Shahzad Murtaza[a], Muhammad Naveed Zafar[c], Bilal Ahmad Khan[d], Sajjad Hussain Sumra[a], Muhammad Nawaz Tahir[e], Kanwal[f], Khalid Mohammed Khan[f,g]

[a]*Department of Chemistry, University of Gujrat, Gujrat 50700, Pakistan*
[b]*Department of Chemistry, Govt. College Women University, Sialkot 51300, Pakistan*
[c]*Department of Chemistry, Quaid-i-Azam University, Islamabad-45320, Pakistan*
[d]*Department of Chemistry, University of Azad Jammu and Kashmir, Muzaffarabad, Pakistan*
[e]*Department of Physics, University of Sargodha, Sargodha, Pakistan*
[f]*H. E. J. Research Institute of Chemistry, International Center for Chemical and Biological Sciences, University of Karachi, Karachi 75270, Pakistan*
[g]*Department of Clinical Pharmacy, Institute for Research and Medical Consultations (IRMC), Imam Abdulrahman Bin Faisal University, P.O. Box 31441, Dammam, Saudi Arabia*

Abstract: The prime objective of this research work is to prepare readily soluble synthetic analogues of naturally occurring 3-*O*-flavonol glycosides and then investigate the influence of various substituents on biological properties of synthetic compounds. In this context, a series of varyingly substituted 3-*O*-flavonol glycosides have been designed, synthesized and characterized efficiently. The structures of synthetic molecules were unambiguously corroborated by IR, ^{1}H-, ^{13}C-NMR and ESI-MS spectroscopic techniques. The structure of compound **22** was also analyzed by X-ray diffraction analysis. All the synthetic compounds (**21**-**30**) were evaluated for *in vitro* inhibitory potential against cholinesterase enzymes. The results displayed that most of the derivatives were potent inhibitors of acetylcholinesterase (AChE) and butyrylcholinesterase (BChE) with varying degree of IC_{50} values. The experimental results were further encouraged by molecular docking studies in order to explore their binding behavior with the active pocket of AChE and BChE enzymes. The experimental and theoretical results are in parallel with one another.

Keywords: Flavonoids, flavonols, 3-hydroxyflavones, glycosides, cholinesterases, AChE/BChE inhibitors, molecular docking studies

*Corresponding Author: ehsan.ullah@uog.edu.pk; Tel.: 0092-333-8464959

Introduction

Flavonoids constitute a large and significant group of naturally occurring secondary metabolites. These ubiquitous compounds play important role in the growth and development of plants, and are beneficial for human health [1,2]. They mostly occur in glycosylated form, comprising an aglycone core and a sugar unit. The attachment of one or more sugar moieties at different positions of the aglycone can give rise to structural variability in these compounds, and thus accountable for increasing their solubility and rendering them to demonstrate their inherent functions such as antioxidant capability and potential biological properties [3] *e.g.*, anticancer, antioxidant and antimicrobial bioactivities [4].

Among these metabolites, flavonol-*O*-glycosides which frequently occur in the form of 3-*O*-glycosides (Figure-1) have attained increasing interest due to their immense medicinal and pharmacological applications. These compounds are reported to possess several pharmacological properties including anticarcinogenic, antiplatelet, antioxidant, antithrombic, antimutagenic, and genoprotective effects, cytoprotective, cardioprotective and vasoprotective activities [5-7]. They also play an important role as interspecies signaling molecules in plants, and in humans they demonstrate a various activities such as antimicrobial, anticancer and radical-scavenging activities [8], antidiarrheic, diuretic, hemostatic, stomachic, uterine congestion, cardiovascular diseases, analgesic, and antidiabetic *etc* [9,10]. Constructive and regulatory functions of these scaffolds are making them intensively investigated class. The modifications are carried out on all the three rings, particularly on ring C, due to which flavonoids represent one of the largest and the most diverse class of plant secondary metabolites [11].

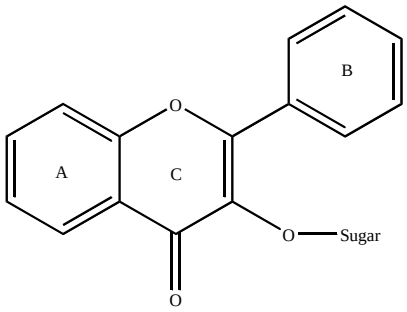

Figure-1: Representative structure of 3-*O*-flavonolglycoside

Alzheimer's disease (AD) is a chronic neurodegenerative disorder characterized by dementia and deficiency in daily life activities along with neuropsychiatric symptoms or behavioral disturbance. The hallmarks of AD are dysfunction of cholinergic system, elevated aggregation of *β*-amyloid peptides (A*β*) and loss of cognitive function [12]. The low level of cholinergic neurotransmission in cortical and other regions of the human brain leads to the loss of cognitive function in AD patients [13]. Studies have shown that by increasing acetycholine (ACh) level through inhibiting acetylcholinesterase (AChE) and butyrylcholinesterase (BChE) enzymes in the body offer a potential therapy for treating AD, and thus improves both mental and memory symptoms in that disease. Standard AChE inhibitors such as donepezil, galantamine, and rivastigmine are involved in improving symptoms for most patients by increasing cholinergic neurotransmission level in the body. However, these drugs are expensive as well as their long term use leads to various adverse side effects and reoccurrence of symtoms [12]. Over the past decades, naturally occurring AChE and BChE inhibitors have been isolated from the plants, and used as natural therapy for AD treatment. In this context, flavonol*O*-glycosides have been reported as potent cholinesterase inhibitors [12-14]. Possible high chelating capability, antioxidant activity and low toxicity of these scaffolds render them promising compounds for developing multipotent drugs against AD [15]. However, natural sources of such drugs are insufficient to cope with requirements all over the globe. Therefore, there is urgent need to explore and design new synthetic analogues of these natural drugs.

In view of immense biological significance of naturally occurring flavonol-3-*O*-glycosides, several workers have reported their isolation from plant sources [16]. The process of isolation and purification of these compounds are quite long, tedious, laborious, expensive, even then small quantities are obtained for testing their biological activities. It is well known that these glycosides are mostly hydroxylated, methoxylated and prenylated at rings A and B. In reality, these substituents are responsible for their reported biological activities. It is also well known that compounds having halogens, nitro, alkyl groups as substituents are also highly bioactive [17,18], nevertheless, in nature no flavonoid glycosides have been reported with these substituent. Therefore, a general synthetic method and combinatorial synthesis of a library of these molecules would be very desirable.

In the light of above-mentioned reports and in order to explore new compounds which might be used as drugs for the treatment of AD and also to find new structures for improving the activity of these scaffolds, we initiated a project aiming to design and synthesize of varyingly substituted acylated flavonol-3-*O*-glycosides in laboratory, since synthesis leads to the target molecules in sufficiently large quantities. Moreover, it is also desire to study the effect of various substituents on cholinesterase inhibitory potential of these compounds, and thus to study the structure activity relationship (SAR) for each of the synthesized compound. The experimental results have also been validated by molecular docking studies.

Material and Methods

All the chemicals were purchased from Merck (Germany) and Sigma-Aldrich (USA) and used as delivered. Melting points were measured on an Electrothermal melting point apparatus and are uncorrected. The IR spectra were recorded on a Bio-red spectrophotometer using KBr discs. NMR spectra were measured on a Bruker DRX 300 instrument (^{1}H, 300 MHz, ^{13}C, 75 MHz). Accurate mass measurements were carried out with the Fisons VG sector-field instrument (EI) and a FT-ICR mass spectrometer. The IR values are mentioned in $\bar{\upsilon}$ units and NMR chemical shift values were determined in ppm units. Absorption spectra

were recorded in dichloromethane on Jasco UV-VIS V-660 or Jasco UV-VIS V-670 instrument. Bruker Smart APEX-II CCD diffractometer was used for single crystal XRD studies.

General Procedure for the synthesis of flavonol 3-*O*-glycosides

Methanolic solution of 2-hydroxyacetophenone (1.2 mL, 10 mmol) was mixed with 10 mL sodium hydroxide (30%) and stirred for 30 min. Benzaldehyde (1.0 mL, 10 mmol) was then added drop wise and the reaction mixture was further stirred for 24 h. Progression of reaction was monitored by comparative TLC. Chalcone so formed was further cyclized by adding 1.5 mL H_2O_2 (35%) followed by stirring for 1 h. After completion, HCl (10%) was added to the reaction mixture and precipitates of flavonol were formed. The precipitate were filtered followed by thoroughly washing with water, the residue obtained was then dried and crystallized from ethanol. Flavonol (238.23 mg, 1.0 mmol) was dissolved in 5.0 mL chloroform containing anhydrous potassium carbonate (414.6 mg, 3.0 mmol), and tetrabutyl ammonium bromide (TBAB 967.0 mg, 3.0 mmol). Then H_2O (5.0 mL) was added drop by drop to the above mixture and stirred for 30 min. Subsequently, peracetylglycosyl bromide (592.0 mg, 1.5 mmol) of was added by further stirring at room temperature for 36 h. The reaction progress was monitored with TLC. The reaction mixture was quenched with the addition of water and neutralized by HCl (10%). The aqueous layer was then extracted with dichloromethane (3×5 mL). The combined organic layer was washed with brine followed by drying over anhydrous sodium sulfate, it was then filtered and concentrated under reduced pressure. The residue was purified by column chromatography through silica gel (pet-ether/ethylacetate (10:1 to 3:1) and furnished the product.

Enzyme Inhibition Essay

Enzyme inhibitory studies were carried out by using Ryan and Ellman method [18] with slight modification. 100 μL of each sample (20, 40, 60, 80, 100 μM) was mixed with 50 μL enzyme (AChE/BChE) and allowed it to stand for 10 minutes. 50 μL of substrate *i.e.*

acetylthiocholine iodide (0.71 mM) for AChE or butyrylthiocholine chloride (0.2 mM) for BChE, 50 μL (0.5 mM) of DTNB [5,5´-dithio-*bis*(2-nitrobenzoic acid)] and 500 μL phosphate buffer of pH 8 added to above mixture and incubated for 20 min at 37 $^{\circ}$C. Solution turned yellow due to formation of 5-thio-2-nitrobenzoate anion as a result of hydrolysis of substrate. The hydrolysis of substrate is monitored spectrophotometrically by measuring absorbance at wavelength of 400 nm and 412 nm for AChE and BChE, respectively. Percentage inhibition was calculated by this formula:

$$(\%)\ \text{Inhibition} = \frac{B-A}{B} \times 100$$

Here A = absorbance of the enzyme with test sample; B = absorbance of enzyme without test sample

Each experiment was repeated thrice and concordant value was used. IC_{50} value was calculated through simple linear regression. Donepezil was used as reference compound.

Molecular Docking Assay [18]

Molecular docking studies were performed to predict the interaction of enzyme and ligand. Crystal structure of AChE and BChE was obtained from (RCSB) protein data bank ACD Chemsketch and 3D Pro 12.0 were used for the 3D optimization of given compounds and were saved as SYBYL mol2 file format. AutoDock Tool v1.5.6 was used for docking, 100 different configurations were optimized. Discovery Studio Visualizerv 4.0 was used for visualization of most potent and best poses of under study compounds.

Results and Discussion

Chemistry

Flavonols (**11-20**) were synthesized starting from 2-hydroxyacetophenone and varyingly substituted aromatic aldehydes in two steps sequence through Algar-Flynn-Oyamada (AFO) reaction [19]. 2'-Hydroxyacetophenone was condensed with various aldehydes in methanolic solution of sodium hydroxide to produce 2'-hydroxychalcones. These intermediate were then oxdatively cyclized with 30% hydrogen peroxide (H_2O_2) in the same solvent under basic

medium to afford 2-hydroxyflavones in excellent yields (Scheme 1). Flavonols so obtained were directly used, without further purification, for the follow-up *O*-glycosylation reaction. The final 3-*O*-glycosylation step was accomplished by treating flavonols with acetobromo-*α*-D-glucose in the presence of potassium carbonate and dimethylformamide (DMF) under phase transfer catalytic conditions.

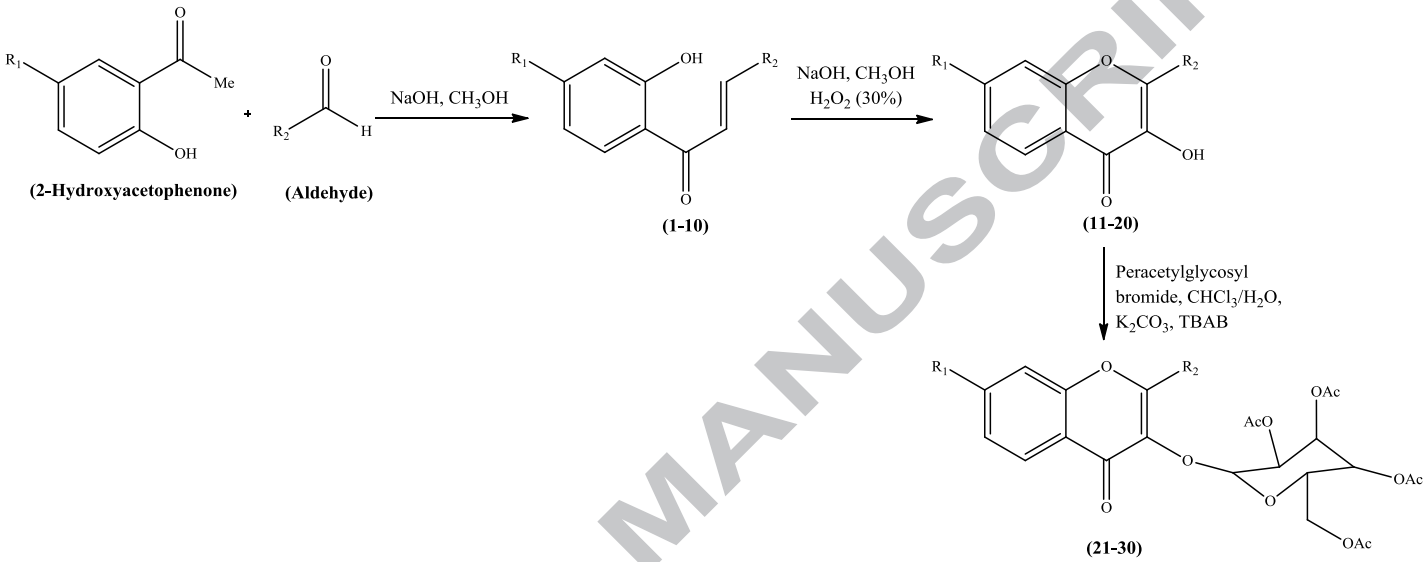

Compound No.	R_1	R_2
21	H	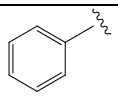
22	H	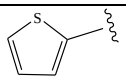
23	H	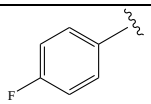
24	H	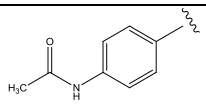
25	H	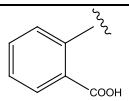
26	H	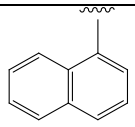

27	H	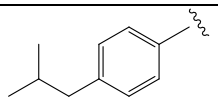
28	H	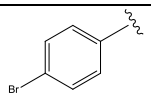
29	H	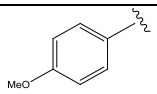
30	CH_3	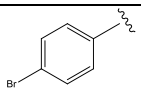

Scheme-1: Synthesis of varyingly substituted 3-*O*-flavonolglycosides (**21-30**)

The target compounds (**21-30**) were synthesized in moderate to excellent yields and were found readily soluble in common organic solvents such as methanol, ethanol, THF, chloroform etc.

All the newly 3-*O*-acylated glycosides were purified by column chromatography and subsequently characterized by FTIR, NMR spectroscopy and mass spectrometry. For instance, in FTIR spectra, the disappearance of peaks around of 3420 cm^{-1} due to 3-OH and appearance of new peaks around 1620 cm^{-1} due to (OAc) indicate successful attachment of acylated sugar with aglycone part. Similarly, ^{1}H-NMR spectra showed the peaks ranging from 8.30 to 7.20 ppm for aromatic protons, the peaks ranging from 6.10 to 4.95 ppm for aliphatic protons of acylated glucose moiety and two singlet peaks at 2.06 and 1.99 ppm for two non-equivalent acetyl groups. Moreover, their ^{13}C-NMR spectra exhibit two characteristics signals around 173 and 170 pmm for flavonol ketonic group and ester acetyl group, respectively. The molecular masses of the 3-*O*-flavonol acylated glycosides were confirmed by electron spray ionization (ESI) mass spectrometry. Their ESI spectra showed quasi molecular ion peaks corresponding to [M+H]. All the spectral data unequivocally corroborate the structures of the newly synthesized molecules. The single crystal for the

compound **22** was grown *via* slow evaporation of dichloromethane solution, and its molecular structure was resolved by X-ray single-crystal structure analysis and is depicted in Figure-2.

a)

b)

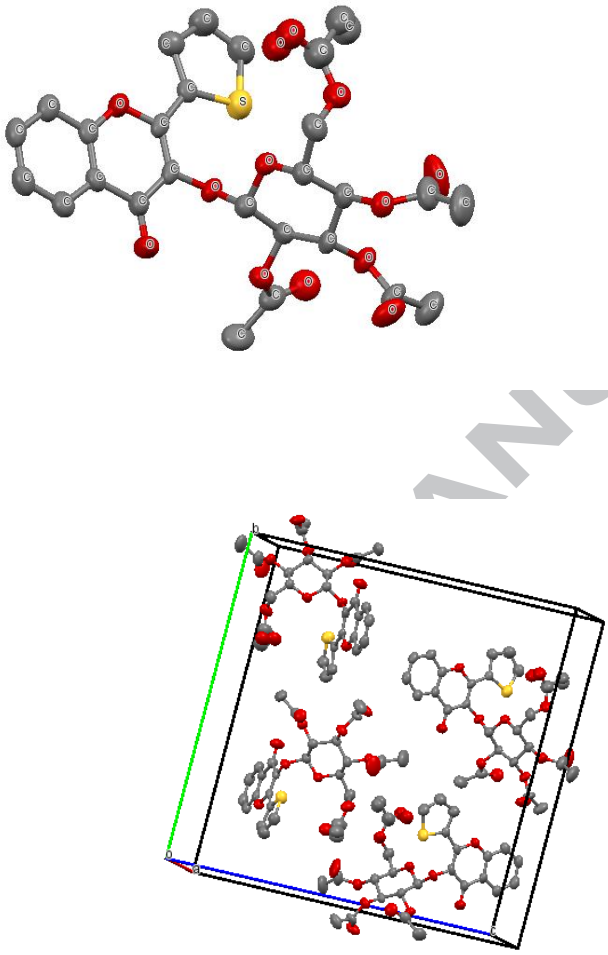

Figure-2: (a) Molecular structure **22**, as determined by X-ray diffraction. Oxygen atoms: red; sulfur: yellow, and hydrogen atoms have been omitted for clarity: (b) 3D view predicting crystal packing pattern.

Crystal data	
CCDC Number	1846188
Chemical Formula	$C_{27}H_{26}O_{12}S$
M_r	574.54

Crystal system, space group	Orthorhombic, $P2_12_12_1$
Temperature (K)	296
a, *b*, *c* (Å)	5.5797 (5), 21.600 (3), 22.668 (3)
V (Å^3)	2732.1 (6)
Z	4
Radiation type	Mo *K*a
m (mm^{-1})	0.18
Crystal size (mm)	0.40 × 0.18 × 0.16
Data collection	
Diffractometer	Bruker Kappa APEXII CCD
Absorption correction	Multi-scan (*SADABS*; Bruker, 2005)
T_{min}, T_{max}	0.910, 0.960
No. of measured, independent and observed [$I > 2s(I)$] reflections	9078, 5286, 2422
R_{int}	0.070
$(\sin q/l)_{max}$ (Å^{-1})	0.617
Refinement	
$R[F^2 > 2s(F^2)]$, $wR(F^2)$, S	0.067, 0.171, 0.96
No. of reflections	5286
No. of parameters	353
No. of restraints	6
H-atom treatment	H-atom parameters constrained
$D\rho_{max}$, $D\rho_{min}$ (e Å^{-3})	0.20, -0.25
Absolute structure	Flack x determined using 954 quotients [(I+)-(I-

	)]/[(I+)+(I-)] (Parsons, Flack and Wagner, Acta Cryst. B69 (2013) 249-259).
Absolute structure parameter	-0.09 (16)

The spectroscopic data of all the newly synthesized target compounds are given below:

2-Phenyl-4*H*-chromen-4-one-3-*O*-2,3,4,6-*O*-tetraacetyl-*β*-D-glucopyranoside (21)

Pale yellow solid; Yield: 70%; m.p. 175-177ºC; IR (ν_{max}; KBr, cm^{-1}): 3112, 2965, 1625, 1507, 1101, 1021; ^{1}H NMR (300 MHz, DMSO-d_6) δ: 9.61 (s, 1H, Ar-H), 8.11 (d, *J* = 8.1 Hz, 1H, Ar-H), 7.79 (m, *J* = 8.7, 1.2 Hz, 1H, Ar-H), 7.74 (d, *J* = 8.4 Hz, 1H, Ar-H), 7.56 (t, *J* = 7.5 Hz, 2H, Ar-H), 7.51 (t, *J* = 7.5 Hz, 1H, Ar-H), 7.46 (t, *J* = 8.7 Hz, 1H, Ar-H), 5.7 (d, *J* = 6.3 Hz, 1H, Aliphatic) 5.31-5.24 (m, 1H, Aliphatic), 5.16 (dd, *J* = 9.6, 6.4 Hz, 1H, Aliphatic), 5.04 (t, *J* = 9.1 Hz, 1H, Aliphatic), 4.38-4.30 (m, 2H, Aliphatic), 4.18-4.11 (m, 1H, Aliphatic), 2.08 (s, 3H, -COH_3), 2.03 (s, 6H, -$COCH_3$), 1.74 (s, 3H, -$COCH_3$); ^{13}C NMR (75 MHz, DMSO-d_6) δ: 175.6, 171.1, 170.6, 170.4, 169.4, 161.1, 158.4, 154.5, 134.4, 134.2, 130.6, 127.0, 124.1, 123.0, 122.4, 118.3, 115.1, 97.5, 70.3, 69.9, 69.4, 67.3, 61.9, 20.7, 20.7, 20.7, 20.6; accurate mass (ESI, AcCN, +ve) of $[M+H]^+$: Calcd for $C_{29}H_{29}O_{12}$ 569.1659; found 569.1645.

Synthesis of 2-(thiophen-2-yl)-4*H*-chromen-4-one 3-*O*-2,3,4,6-*O*-tetraacetyl-*β*-D-glucopyranoside (22)

Light yellow solid; Yield: 78%; m.p. 185-186 °C; IR (ν_{max}; KBr, cm^{-1}): 3104, 2971, 1614, 1502, 1112, 1035; ^{1}H NMR (300 MHz, DMSO-d_6) δ: 8.17-7.97 (m, 3H, Ar-H), 7.92-7.69 (m, 2H, Ar-H), 7.52 (d, *J* = 1.01 Hz, 1H, Ar-H), 7.32 (dd, *J* = 4.95, *J* = 3.85 Hz, 1H, Ar-H), 6.06 (d, *J* = 7.70 Hz, 1H, Aliphatic), 5.44 (d, *J* = 9.54 Hz, 1H, Aliphatic), 5.35-5.21 (m, 1H, Aliphatic), 5.05-4.90 (m, 1H, Aliphatic), 3.97-3.89 (m, 2H, Aliphatic), 2.06 (s, 3H, -COH_3), 1.99 (s, 6H, -$COCH_3$), 1.70 (s, 3H, -$COCH_3$); ^{13}C NMR (75 MHz, DMSO-d_6) δ: 172.2, 169.8, 169.7, 169.6, 169.4, 154.5, 152.3, 134.6, 133.3, 133.2, 131.5, 131, 127.9, 125.5, 125.1,

123.4, 118.4, 97.8, 72.2, 71.8, 70.9, 68.1, 60.9, 20.7, 20.6, 20.5, 20.2; accurate mass (ESI, AcCN, +ve) of $[M+H]^+$: Calcd for $C_{27}H_{27}O_{12}S$ 575.1223; found 575.1205.

2-(4-Flourophenyl)-4*H*-chromen-4-one-3-*O*-2,3,4,6-*O*-tetraacetyl-*β*-D-glucopyranoside (23)

Off-white solid; Yield: 66%; m.p. 171-173 °C; IR (ν_{max}; KBr, cm^{-1}): 3110, 2970, 1615, 1512, 1115, 1015; ^{1}H NMR (300 MHz, DMSO-d_6) δ: 8.23-8.05 (m, 3H, Ar-H), 7.87 (ddd, J = 8.48, 6.92, 1.65 Hz, 1H, Ar-H), 7.77 (dd, J = 8.44, 0.73 Hz, 1H Ar-H), 7.54 (ddd, J = 7.98, 6.97, 1.19 Hz, 1H, Ar-H), 7.47-7.32 (m, 2H Ar-H), 5.73 (d, J = 7.89 Hz, 1H, Aliphatic), 5.48-5.31 (m, 1H, Aliphatic), 5.11-4.82 (m, 3H, Aliphatic), 4.02-3.77 (m, 3H, Aliphatic), 2.07 (s, 3H, -$COCH_3$), 1.97 (s, 6H, -$COCH_3$), 1.82 (s, 3H, $COCH_3$); ^{13}C NMR (75 MHz, DMSO-d_6) δ: 173.3, 170.1, 169.9, 169.7, 156.3, 155.2, 136.2, 132.1, 132, 127.2, 125.8, 123.8, 119, 115.9, 115.6, 98.9, 72.2, 71.8, 71, 68.3, 61.5, 20.9, 20.8, 20.6, 20.4; accurate mass (ESI, AcCN, +ve) of $[M+H]^+$: Calcd for $C_{29}H_{28}O_{12}F$ 587.1564; found 587.1551.

2-(4-Acetamidophenyl)-4*H*-chromen-4-one-3-*O*-2,3,4,6-*O*-tetraacetyl-*β*-D-glucopyranoside (24)

Yellow solid; Yield: 75%; m.p. 200-203 °C; IR (ν_{max}; KBr, cm^{-1}): 3310, 3104, 2981, 1620, 1520, 1117, 1011; ^{1}H NMR (300 MHz, DMSO-d_6) δ: 8.37-8.25 (m, 1H, N -H), 8.22-8.12 (m, 1H, Ar-H), 7.75 (dd, J = 7.79, 1.56 Hz, 1H, Ar-H), 7.61 (d, J = 8.62 Hz, 1H, Ar-H), 7.45-7.30 (m, 1H, Ar-H), 6.88-6.73 (m, 2H, Ar-H), 6.54 (d, J = 8.8 Hz, 1H, Ar-H), 6.06 (d, J = 7.70 Hz, 1H, Aliphatic), 5.44 (d, J = 9.54 Hz, 1H, Aliphatic), 5.35-5.21 (m, 1H, Aliphatic), 5.05-4.90 (m, 1H, Aliphatic), 3.97-3.89 (m, 2H, Aliphatic), 2.02 (s, 3H, -$COCH_3$), 1.98 (s, 6H, -$COCH_3$), 1.70 (s, 3H, -$COCH_3$), 1.23 (s, 3H, Aliphatic); ^{13}C NMR (75 MHz, DMSO-d_6) δ: 171.8, 169.8, 169.4, 169.2, 167.4, 165.8, 161.6, 153.1, 150, 134.2, 131.2, 130.7, 130.1, 123.7, 118.1, 116.6, 112.5, 96.3, 72.2, 71.7, 71.2, 68, 62.4, 21.9, 20.6, 20, 20.5, 20.8; accurate mass (ESI, AcCN, +ve) of $[M+H]^+$: Calcd for $C_{31}H_{32}O_{13}N$ 626.1873; found 626.1850.

2-(2-Carboxyphenyl)-4H-chromen-4-one-3-*O*-2,3,4,6-*O*-tetraacetyl-*β*-D-glucopyranoside (25)

Light yellow solid; Yield: 45%; m.p. 230-233 °C; IR (ν_{max}; KBr, cm^{-1}): 3450, 3108, 2988, 1619, 1526, 1109, 1030; ^{1}H NMR (300 MHz, DMSO-d_6) δ: 8.04 (dd, J = 8.1, 1.5 Hz, 1H, Ar-H), 7.84 (ddd, J = 20, 7.8, 1.6 Hz, 2H, Ar-H), 7.75-7.61 (m, 3H, Ar-H), 7.54 (ddd, J = 8.3, 7.2, 1.4 Hz, 1H, Ar-H), 7.46 (ddd J = 7.6, 1.7 Hz, Ar-H), 5.79 (d, J = 6.4 Hz, 1H, Aliphatic), 5.82 (dd, J = 9.5, 9 Hz, 1H, Aliphatic), 5.1-5 (m, 2H, Aliphatic), 4.39-4.31 (m, 2H), 4.18-4.11 (m, 1H, Aliphatic), 2.10 (s, 3H, -$COCH_3$), 2.05 (s, 6H, -$COCH_3$), 1.75 (s, 3H, -$COCH_3$); ^{13}C NMR (75 MHz, DMSO-d_6) δ: 192.4, 170.6, 168.7, 168.5, 168, 166.5, 141, 140.8, 136.4, 132.7, 125.9, 124.4, 123.6, 117.8, 113.7, 98.9, 71.6, 71.1, 71, 69.1, 62.4, 22.3, 20.6, 20.3, 20.2, 20.1; accurate mass (ESI, AcCN, -ve) of $[M-H]^-$: Calcd for $C_{30}H_{27}O_{14}$ 611.1400; found 611.1390.

2-(Naphthalen-1-yl)-4*H*-chromen-4-one-3-*O*-2,3,4,6-*O*-tetraacetyl-*β*-D-glucopyranoside (26)

Off-white solid; Yield: 73%; m.p. decompose above 185 °C; IR (ν_{max}; KBr, cm^{-1}): 3141, 3011, 1627, 1536, 1107, 1038; ^{1}H NMR (300 MHz, DMSO-d_6) δ**:** 8.26-8.17 (m, 1H, Ar-H), 8.04 (dd, J = 8.1, 1.5 Hz, 1H, Ar-H), 7.95-7.86 (m, 3H, Ar-H), 7.71 (dd, J = 8.3, 1.3 Hz, 1H, Ar-H), 7.65 (ddd, J = 8.3, 7.1, 1.5 Hz, 1H, Ar-H), 7.61-7.51 (m, 2H, Ar-H), 7.53-7.43 (m, 2H, Ar-H), 5.5 (d, J = 6.0 Hz, 1H, Aliphatic), 5.44 (m, J = 9.54 Hz, 1H, Aliphatic), 5.21-5.35 (m, 1H, Aliphatic), 4.9-5.05 (m, 1H, Aliphatic), 3.99-3.98 (m, 2H, Aliphatic), 2.08 (s, 3H, -COH_3), 1.95 (s, 6H, -$COCH_3$), 1.74 (s, 3H, -$COCH_3$); ^{13}C NMR (75 MHz, DMSO-d_6) δ: 173.5, 170.6, 170.2, 169.6, 159.1, 155.8, 138.1, 135.0, 133.5, 131, 128, 126.8, 124.4, 119.1, 99.2, 89.5, 72.8, 72.2, 71.6, 71.0, 69.0, 66.8, 61.6, 60.8, 29.5, 21, 21, 20.8, 20.7, 14; accurate mass (ESI, AcCN, +ve) of $[M+H]^+$: Calcd for $C_{33}H_{30}O_{12}$ 618.1737; found 618.1708.

2-(4-Isobutylphenyl)-4*H*-chromen-4-one-3-*O*-2,3,4,6-*O*-tetraacetyl-*β*-D-glucopyranoside (27)

Light yellow solid; Yield: 83%; m.p. 172-175 °C; IR (ν_{max}; KBr, cm^{-1}): 3110, 2990, 1643, 1516, 1112, 1023; ^{1}H NMR (300 MHz, DMSO-d_6) δ: 8.15 (m, 1 H, Ar-H), 8.12 (d, J = 3.0 Hz, 1H, Ar-H), 7.97 (m, 1H, Ar-H), 7.49 (d, J = 6.0 Hz, 1H, Ar-H), 7.47 (d, J = 3.0 Hz, 1H, Ar-H), 5.5 (d, J = 6 Hz, 1H, Aliphatic), 5.44 (m, J = 9.5 Hz, 1H, Aliphatic), 5.35-5.21 (m, 1H, Aliphatic), 5.05-4.90 (m, 1H, Aliphatic), 3.99-3.90 (m, 2H, Aliphatic), 2.40 (d, J = 9.0 Hz, 2 H, Aliphatic), 2.08 (s, 3H, -COH_3), 1.95 (s, 6H, -$COCH_3$), 1.92 (s, 3H, -$COCH_3$), 1.90 (m, 1 H, -CH-), 1.74 (d, J = 9.0 Hz, 2H, -CH_2-) 1.05 (d, J = 9.0 Hz, 6 H, -$(CH_3)_2$); ^{13}C NMR (75 MHz, DMSO-d_6) δ: 192.2, 168.8, 169.5, 169.3, 161.7, 142.5, 136.2, 136, 129.6, 127.0, 126.0, 121.6, 121.0, 119.0, 118.0, 98.4, 79.6, 71.5, 71.2, 70.6, 68.6, 67.3, 62.3, 45.1, 44.6, 30.2, 29.8, 28.3, 23.2, 22.4, 22.3, 20.4, 20.2, 20.2, 13.8, 10.7; accurate mass (ESI, AcCN, +ve) of $[M+H]^+$: Calcd for $C_{33}H_{37}O_{12}$ 625.2285; found 625.2274.

2-(4-Bromophenyl)-4*H*-chromen-4-one-3-*O*-2,3,4,6-*O*-tetraacetyl-*β*-D-glucopyranoside (28)

Yellow solid; Yield: 63%; m.p. 190-192 °C; IR (ν_{max}; KBr, cm^{-1}): 3112, 2967, 1620, 1524, 1117, 1018; ^{1}H NMR (300 MHz, DMSO-d_6) δ: 8.3 (s, 1H, Ar-H), 8.1 (d, J = 15.0 Hz, 2H, Ar-H), 7.8-7.6 (m, 3H, Ar-H), 7.55-7.40 (m, 2H, Ar-H), 5.8 (dd, J = 9.0, 3.0 Hz, 1H, Aliphatic), 5.45-5.35 (m, 1H, Aliphatic), 5.05-4.85 (m, 4H, Aliphatic), 2.11 (s, 3H, -COH_3), 1.97 (s, 6H, -$COCH_3$), 1.72 (s, 3H, -$COCH_3$); ^{13}C NMR (75 MHz, DMSO-d_6) δ: 173.0, 169.6, 169.2, 167.0, 155.0, 154.7, 136.1, 133.5, 132.3, 131.3, 130.3, 128.0, 125.3, 123.3, 121.3, 118.6, 98.4, 71.6, 71.3, 70.6, 67.8, 67.3, 61.2, 29.8, 28.3, 23.2, 22.3, 20.4,20.2, 20.2; accurate mass (ESI, AcCN, +ve) of $[M+H]^+$: Calcd for $C_{29}H_{27}O_{12}Br$ 646.0685 (monoisotopic); found 646.0660.

2-(4-Methoxyphenyl)-4*H*-chromen-4-one-3-*O*-2,3,4,6-*O*-tetraacetyl-*β*-D-glucopyranoside (29)

Yellowish green solid; Yield: 70%; m.p. 169-171 °C; IR (ν_{max}; KBr, cm^{-1}): 3123, 2991, 1601, 1530, 1124, 1037; ^{1}H NMR (300 MHz, DMSO-d_6) δ: 8.03 (dd, J = 8.1, 1.5 Hz, 1H, Ar-H), 8.01-7.95 (m, 2H, Ar-H), 7.7 (dd, J = 8.2, 1.4 Hz, 1H), 7.65 (ddd, J=8.3, 7.1, 1.5 Hz, 1H, Ar-H), 7.54 (ddd, J = 8.3, 7.1, 1.4 Hz, 1H, Ar-H), 7.25-7.19 (m, 2H, Ar-H), 5.6 (dd, J = 8.0, 3.0 Hz, 1H, Aliphatic), 5.55-5.45 (m, 1H, Aliphatic) 5.20-4.90 (m, 4H, Aliphatic), 3.84 (s, 3H, OMe), 2.11 (s, 3H, -COH_3), 1.97 (s, 6H, -$COCH_3$), 1.76 (s, 3H, -$COCH_3$); ^{13}C NMR (75 MHz, DMSO-d_6) δ**:** 175.6, 171.1, 170.6, 170.4, 169.4, 161.1, 158.4, 154.5, 134.4, 134.2, 131.2, 126.9, 124.1, 122.9, 122.4, 118.3, 115.1, 97.5, 70.3, 69.9, 69.4, 67.3, 61.9, 55.8, 55.3, 20.7, 20.7, 20.7, 20.6; accurate mass (ESI, AcCN, +ve) of $[M+H]^+$: Calcd for $C_{30}H_{31}O_{13}$ 599.17646; found 599.1740.

7-Methyl-2-(4-bromophenyl)-4*H*-chromen-4-one-3-*O*-2,3,4,6-*O*-tetraacetyl-*β*-D-glucopyranoside (30)

Yellow solid; Yield: 75%; m.p. 194-196 °C; IR (ν_{max}; KBr, cm^{-1}): 3105, 2960, 1601, 1503, 1098, 1026; ^{1}H NMR (300 MHz, DMSO-d_6) δ: 8.05-7.97 (m, 2H, Ar-H), 7.86 (d, J = 8.4 Hz, 1H), 7.70 (d, J = 2.2 Hz, 1H), 7.61-7.52 (m, 3H, Ar-H), 7.42 (dd, J = 8.4, 2.2 Hz, 1H, Ar-H), 5.81 (d, J = 6.4 Hz, 1H, Aliphatic), 5.28 (dd, J = 9.5, 3.0 Hz, 1H), 5.13 (dd, J = 9.5, 6.4 Hz, 1H), 5.04 (t, J = 9.1 Hz, 1H, Aliphatic), 4.38-4.30 (m, 2H, Aliphatic), 4.18-4.11 (m, 1H, Aliphatic), 2.50 (s, 3H, Me), 2.11 (s, 3H, -COH_3), 1.97 (s, 6H, -$COCH_3$), 1.72 (s, 3H, -$COCH_3$); ^{13}C NMR (75 MHz, DMSO-d_6) δ: 175.6, 171.1, 170.6, 170.4, 169.4, 158, 154.8, 134.2, 130.6, 130.4, 129.2, 128.6, 128.2, 127.5, 124, 123.8, 120.1, 97.5, 71.3, 70.6, 67.8, 67.3, 61.2, 20.8, 20.4, 20.2, 20.2, 20.0; accurate mass (ESI, AcCN, +ve) of $[M+H]^+$: Calcd. for $C_{30}H_{31}O_{12}$ 662.0998 (monoisotopic); found 662.0970.

Cholinesterase Enzymes Inhibition Assay

In continuation to our efforts on enzyme inhibition studies [18], all the target compounds (**21-30**) were screened *in vitro*, for their inhibitory potential against commercially available electric eel acetylcholinesterase (AChE) and horse serum butrylcholinesterase (BChE) enzymes by using spectrophotometric method.

The experimental results are reported in Table 1. Their IC_{50} values were also calculated, and Donepezil was used as standard.

Table-1: Cholinesterase inhibition efficacy of compounds **21-30**

Compound No.	**Compound Structure**	**AChE IC_{50} ± SEM[a] (μM)**	**BChE IC_{50} ± SEM[a] (μM)**
21	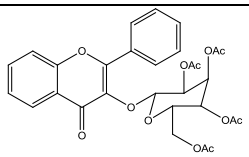	102.91±0.96	45.86±0.39
22	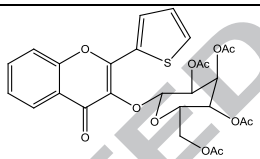	18.52±0.81	25.51±0.08
23	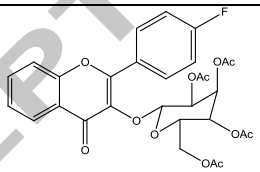	29.23±0.56	49.83±0.72
24	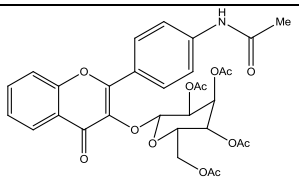	38.70±0.00	39.70±0.87
25	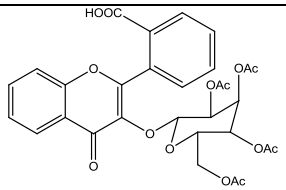	34.05±0.01	48.43±0.03

26	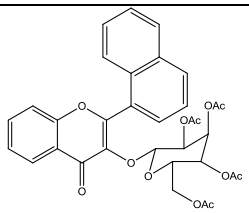	36.35±1.30	18.69±0.01
27	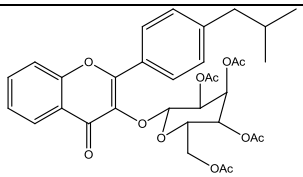	02.05±0.11	05.42±0.33
28	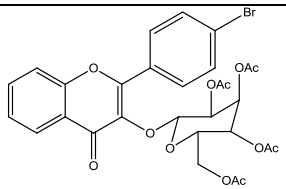	10.20±0.10	03.12±0.35
29	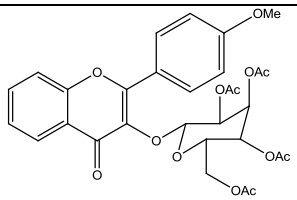	20.70±0.15	26.00±0.16
30	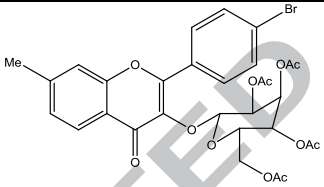	22.36±0.10	30.58±0.18
Donepezil[St]	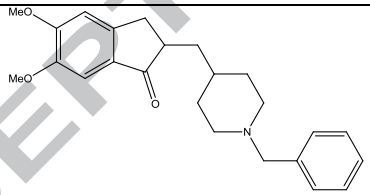	0.09±0.19	0.13±0.22

[a]IC_{50} values (mean ± standard error of mean); [St]Standard inhibitor for AChE and BChE enzymes

All the tested derivatives (**21-30**) displayed potent variable degree of inhibition (IC_{50} = 02.05 ± SEM to 102.91 ± SEM μM) as compared to standard drug donepezil (IC_{50} = 0.09 ± SEM (AChE) and 0.13 ± SEM μM (BChE). Most of the derivatives are potent selective inhibitor of either AChE or BChE enzyme. The experimental results showed that these compounds are comparatively more inhibitor for AChE as compared to BChE. This is attributed to relatively smaller active site of AChE enzyme that can assimilate the smaller groups unlike the larger

active site of BChE enzyme. Even though all the structural features were actively taking part in inhibitory activity, however, the variation of different groups on main structural motif was actually accountable for alteration in inhibitory potential. The compound **27** was found to be the most active dual inhibitor (IC_{50} = 02.05 μM for AChE and 05.42 μM for BChE) among the series having isobutyl at 4' position of the phenyl ring. The high inhibitory potential of this compound is mainly due to hydrophobic interactions of that alkyl group with non-polar pockets of the envisioned enzymes. The next most potent dual inhibitor is compound **28** ((IC_{50} = 10.20 μM for AChE and 03.12 μM for BChE) with bromo group at 4' position of the phenyl ring. This derivative is relatively selective for BChE. Its inhibitory potential is due to the formation of strong non-bonding interactions with active pockets of the envisioned enzymes. The un-substituted derivative **21** was appeared to be about least inhibitor against both enzymes among the series (Table-1). This reflects the fact that mostly inhibitor potential of these compounds is due to the presence of different substituents on the main scaffold. Overall, it has been observed that all the compounds (**21-30**) are comparatively better potent inhibitor against AChE as compare to BChE (Table-1). These results showed that substitution at the ring B increase the inhibitory potential of these compounds in comparison to un-substituted compound **21**. Moreover, sulfur containing ring, for example compound **22**, makes strong interaction with active pockets of AChE (IC_{50} = 18.52 μM) rather than BChE (IC_{50} = 25.51 μM). It is noted that proper substitution on the ring A, B and glycosylation control the activity of these compounds against cholinesterase enzymes. Since, all envisioned compounds have common 3-*O*-glycosylated flavone skeleton in their structures; the activity was mainly due to different functional groups attached on the main framework of flavonol. These findings have been further studied by *in silico* studies (molecular docking). These results manifest that such multifunctionalized structural motifs are promising candidates for designing and the development of new scaffolds for the cure of Alzheimer disease.

Molecular Docking Studies

All the compounds (**21-30**) were analyzed by molecular docking studies in order to find out plausible binding interactions of inhibitors with the active pocket sizes of the enzymes, and also to figure out protein-ligand interactions at molecular level for establishing SAR studies. For this studies, X-ray structures of human AChE (PDB ID: 4BDT) and BChE (PDB ID: 4BDS) were selected as templates. The lowest bonding energies of the compounds (**21-30**) obtained after docking analyzing are given in Table-2.

Table-2: Binding energies of selective posses against human AChE and BChE

Compound No.	***h* AChE Lowest Binding Energy ΔG in KJ mol^{-1}**	***h* BChE Lowest Binding Energy *Δ*G in KJ mol^{-1}**
21	-6.04	-8.81
22	-5.06	-8.40
23	-5.32	-9.08
24	+2.38	-8.38
25	-0.37	-7.97
26	+0.96	-8.97
27	-8.24	-9.48
28	-3.93	-8.98
29	+1.05	-8.71
30	+0.55	-9.81
Standard	-10 (HUW)	-6.83 (THA)

The docking analysis demostrated the top ranked conformations of all compounds were well accommodated inside the active site of AChE and BChE enzymes and comprised of different types of interactions with the active site residues of the envisioned enzymes. For instance, the visualization of compound **22** inside the active pockets of human AChE enzyme revealed

several important interactions as shown in Figure-3. This compound forms hydrogen bonding interaction with amino acid residues Tyr124, Gly121, Ser125, Tyr337, hydrophobic π-alkyl interactions with Trp86 and hydrophobic π-π stacked interactions with Trp439, Tyr337, and Trp86. Moreover, π-lone pair interactions with Trp86 and π-sulfur interactions with MET443, Tyr341 are involved with AChE enzyme.

Similarly, the visualization of the same potent compound **22** showed several important interactions inside the active pocket of BChE enzyme as displayed in Figure-4. This derivative establishes H-bonding with amino acid residues Pro285, Ser198, hydrophobic π-π T shaped interactions with Trp82, Trp231, hydrophobic amide-π stacked interactions with Gly116 and π-sulfur interactions with Trp231 inside the active pocket of human BChE.

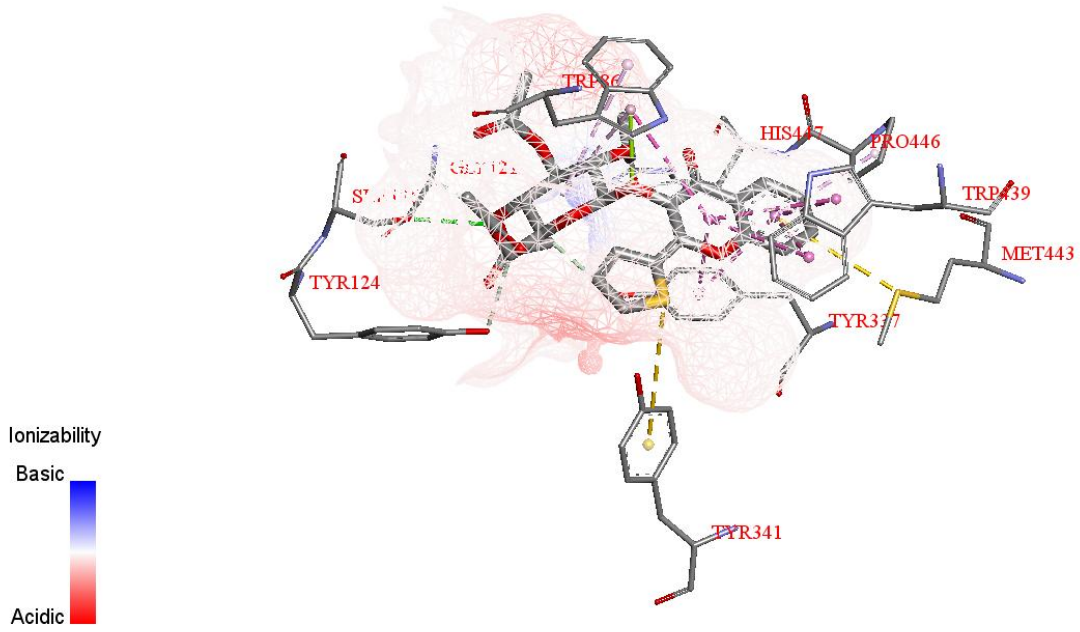

Figure-3: Putative binding interactions of compound **22** against AChE

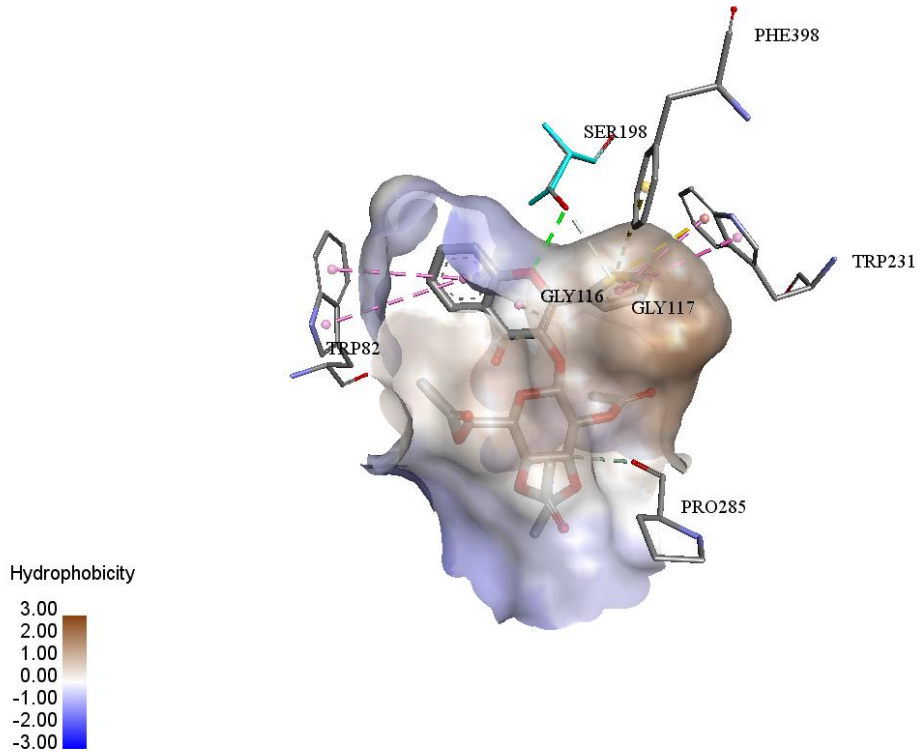

Figure-4: Putative binding interactions of compound **22** against BChE

Furthermore, visualization of most potent compound **27** shows hydrogen bonding with amino acid residues of catalytic triad of AChE, as 'O' atom of Ser125 form hydrogen bond with acetyl group of glycone portion of under observed compound. This compound also shows hydrogen bonding with Tyr341. The overall this derivative shows hydrophobic π-π stacked interaction with Met443, Trp86, Tyr337 with AChE. Trp86 shows hydrophobic π-π T-shaped, hydrophobic π-alkyl type of interaction with AChE. Tyr133 shows hydrophobic π-alkyl type interaction with manifested compound as depicted in Figure-5.

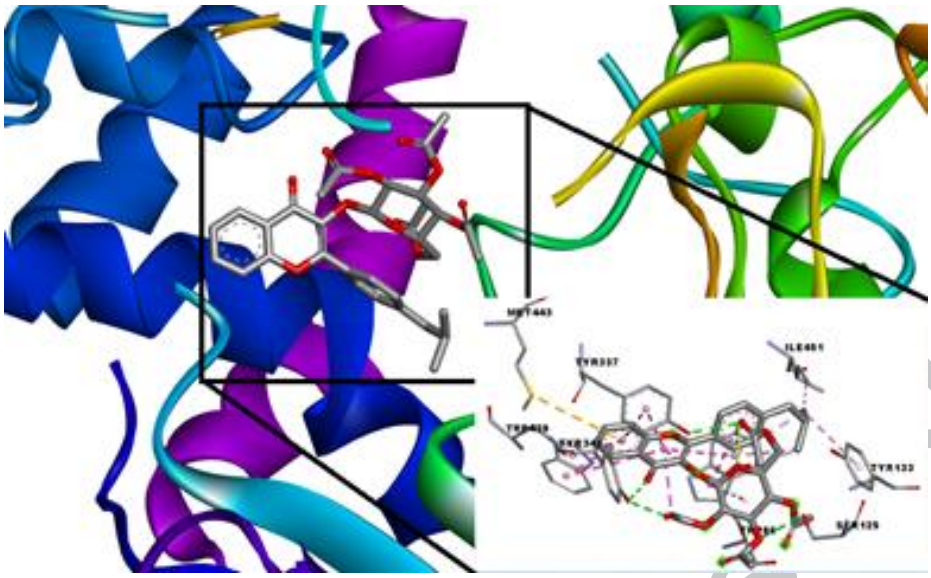

Figure-5. Interactions of the compound **27** with AChE at 3D space. Interactions with specific amino acid residues are shown in the box. The 3D ribbon represents the enzyme, stick model is the lowest energy conforms of the inhibitor **27** along with amino acids of AChE interacting with it.

In continuation, the carbonyl group of other potent compound **27** present in the ring C shows hydrogen bonding with catalytic triad amino acid residue Ser198 inside BChE. Glycone portion of given compound reveals its inhibitory potential by developing hydrogen bonding with catalytic triad (His438) of BChE. Gly116, Gly117 of oxyanion hole also shows hydrophobic amide π-stacked interaction with this ligand in BChE. Leu286 of acyl binding site of BChE exhibit hydrophobic π-alkyl association with this compound. Trp82 of peripheral anionic site (PAS) shows hydrogen bonding with the glycone portion of envisioned compound. Overall Phe329 and Trp82 of BChE shows hydrophobic π-π T- shape and π-sigma type forces of attractions, respectively, with this ligand as shown in Figure-6.

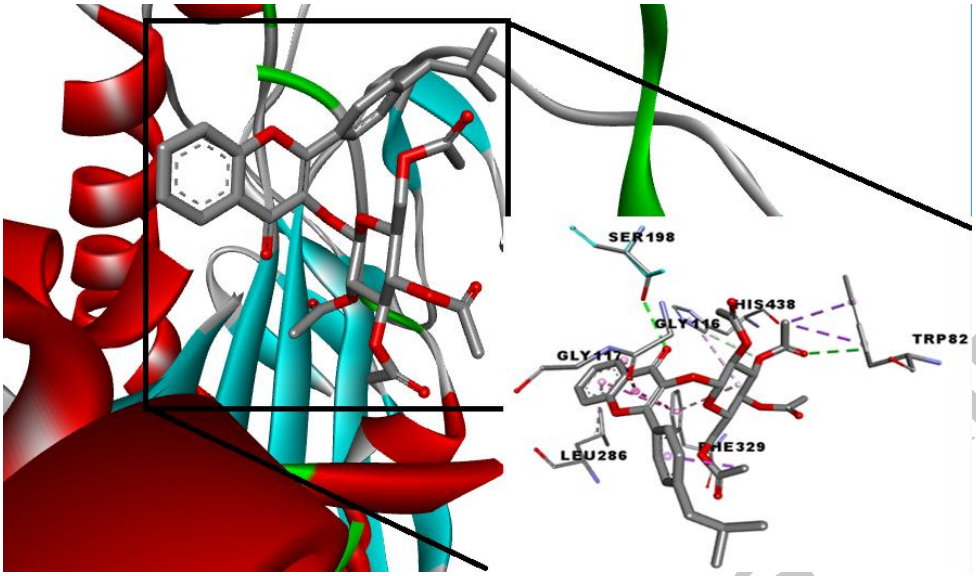

Figure-6. Interactions of the compound **27** with BChE at 3D space. Interactions with specific amino acid residues are shown in the box. The 3D ribbon represents the enzyme, stick model is the lowest energy conforms of the inhibitor **27** along with amino acids of BChE interacting with it.

Moreover, docking studies of compound **28** against AChE reveals several types of associations. Thr83, Ser125, Gly121, Gly122 shows hydrogen bonding with that ligand. Trp 86 of catalytic triad of AChE shows hydrophobic π-π T-shaped association with ligand **28**. This compound also exhibits hydrophobic π-π stacked type of associations with amino acid residue Trp439 and Tyr337. Additionally, this shows hydrophobic π-alkyl interaction with Pro446 and Trp86. Met443 shows π-sulfur type of associations with ligand **28** inside the active pocket of AChE enzyme. The interaction mode has been shown in Figure-7.

Similarly, the ligand **28** expresses its inhibitory potential against BChE by showing π-lone pair interaction with Trp82 of peripheral anionic site (PAS) with 'O' atom of acetyl group of the ligand. Gly117 of oxyanion hole shows hydrogen bonding with the ligand **28**. Leu286 of acyl binding site shows hydrophobic π-alkyl interaction with aromatic ring A of under study compound. His438 of catalytic triad shows hydrophobic π-alkyl interaction with glycone portion of this ligand. Overall Trp231 and Phe329 exhibit hydrophobic π-π T-shaped type of interactions with the **28** as depicted in Figure-8.

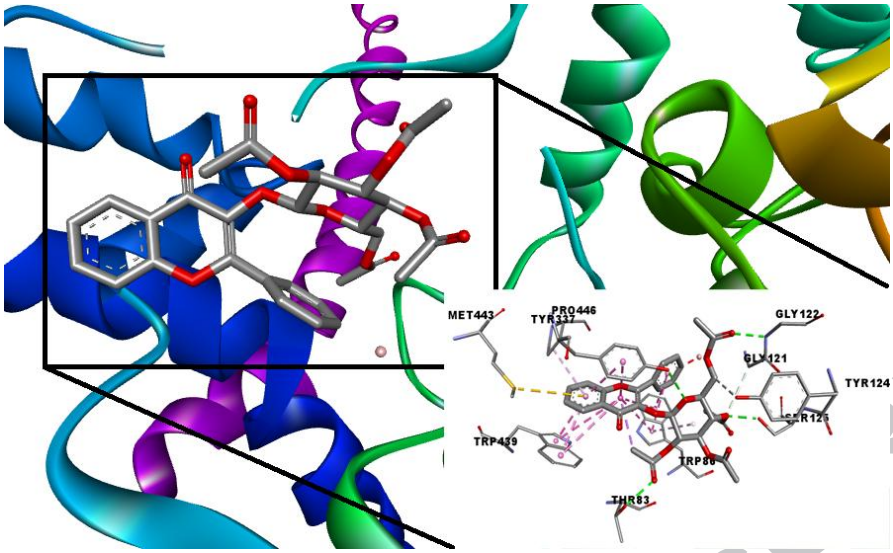

Figure-7. Interactions of **28** with AChE at 3D space. Interactions with specific amino acid residues are shown in the box. The 3D ribbon represents the enzyme, stick model is the lowest energy conforms of the inhibitor **28** along with amino acids of AChE interacting with it.

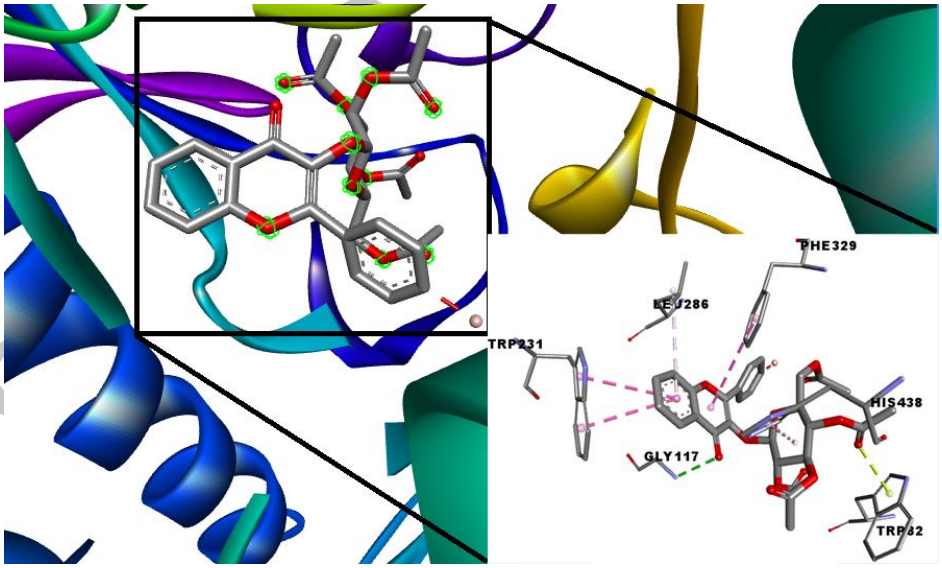

Figure-8. Interactions of **28** with BChE at 3D space. Interactions with specific amino acid residues are shown in the box. The 3D ribbon represents the enzyme, stick model is the lowest energy conforms of the inhibitor **28** along with amino acids of BChE interacting with it.

Conclusion

In conclusion, an efficient synthesis, characterization and biological evaluation of 3-*O*-flavonol glycosides as potent AChE and BChE inhibitors have been reported. The compounds **21-30** were synthesized starting from 2-hydroxyacetophenone and varyingly substituted aromatic aldehydes by employing literature known procedures after little modifications. These derivatives were screened for their potential against cholinesterase enzymes. Enzymes inhibition assay revealed that most of the compounds are relatively more activity against AChE in comparison to BChE. The SAR studies were established on the basis of substitution pattern on flavonol scaffold. The experimental results were further supported by molecular docking analysis. The theoretical results are in accordance with experimental results. These findings have paved the way to design and develop new potent cholinesterase enzymes inhibitor on the basis of 3-*O*-flavonol glycosides for the treatment of Alzheimer disease, and thus may also be of interest for applications in medicinal chemistry.

Acknowledgements

The financial support for this work is gratefully acknowledged by Higher Education Commission of Pakistan under the SRGP Project. 282 and NRPU Project. 6484. Also, we are thankful to Prof. Dr. Lukas J. Gooßen, Department of Chemistry, Bochum University, Germany for his kind help in getting spectroscopic measurements.

References

1. Bohm, B. A. *Introduction to Flavonoids*; Harwood Academic Publishers: Amsterdam, 1998.
2. Ren, G.; Hou, J.; Fang, Q.; Sun, H.; Liu, X.; Zhang, L.; Wang, P. G.; Synthesis of flavonol 3-*O*-glycoside by UGT78D1, *Glycoconj J.,* **2012**, *29,* 425-432, and references quoted therein.

3. Jones, P.; Messner, B.; Nakajima, J.-I.; Schäffner, A. R.; Saito, K., UGT73C6 and UGT78D1, glycosyltransferase involved in flavonol glycoside biosynthesis in Arabidopsis thliana. *J. Biol. Chem.* **2003**, 278(45), 43910-43918.

4. Harborne, J. B.; Baxter, H. *The Handbook of Natural Flavonoids*;John Wiley & Sons: Chichester, 1999; Vol. 1.

5. Chua, L. S. A review on plant-based rutin extraction methods and its pharmacological activities. *J. Ethnopharmacol.* **2013**, 150(3), 805-817.

6. Bhouri, W.; Sghaier, M. B.; Kilani, S.; Bouhlel, I.; Dijoux-Franca, M. G.; Ghedira, K.; Evaluation of antioxidant and antigenotoxic activity of two flavonoids from Rhamnusalaternus L. (Rhamnaceae): kaempferol 3-*O*-*β*-isorhamninoside and rhamnocitrin 3-*O*-*β*-isorhamninoside. *Food Chem. Toxicol.* **2011**, 49(5), 1167-1173.

7. Bhouri, W.;Boubaker, J.;Kilani, S.; Ghedira, K.; Chekir-Ghedira, L.; Flavonoids from Rhamnusalaternus L. (Rhamnaceae): Kaempferol 3-*O*-*β*-isorhamninoside and rhamnocitrin 3-*O*-*β*-isorhamninoside protect against DNA damage in human lymphoblastoid cell and enhance antioxidant activity. *S. Afr. J. Bot.* **2012**, 80 (0), 57-62.

8. Yang,W.; Sun, J.; Lu, W.; Li, Y.; Shan, L.; Han,W.; Zhang, W-D.; Yu, B. Synthesis of Kaempferol 3-*O*-(300,600-di-*O*-*E*-*p*-coumaroyl)-*β*-D-glucopyranoside, efficient glycosylation of flavonol 3-OH with glycosyl *o*-alkynylbenzoates as donors, *J. Org. Chem.* **2010**, *75*, 6879-6888.

9. Veitch, N. C.; Grayer, R. J.; Di, C.; Grayer, R. J.; Grayer, J. Flavonoids and their glycosides, including anthocyanins. *Nat. Prod. Rep.* **2011**, *28*, 1626-1695.

10. (a) Arima, H.; Danno, G. Isolation of antimicrobial compounds from guava (Psidiumguajava L.) and their structural elucidation, *Biosci. Biotechnol. Biochem.* **2002**, *66*, 1727-1730. (b) Cardenas, L.; Rodriguez, J.; Villaverd, M.; Riguera, R.;

Cadena, R.; Otero, J., The analgesic activity of hedyosmumbonplandianum: flavonoid glycosides, *Planta Medica*, **1993,** *59*, 26-27.

11. Culhaoglu, B.; Capan, A.; Boga, M.; Ozturk, M.; Ozturk, T.; Topcu, G. Antioxidant and anticholinesterase activities of some dialkylamino substituted 3-hydroxyflavone derivatives, *Med. Chem.* **2017**, *13*, 1-6.
12. Balkis, A.; Tran, K.; Lee, Y. Z.; Ng, K. Screening flavonoids for inhibition of acetylcholinesterase identified baicalein as the most potent inhibitor, *J. Agric. Sci.* **2015**, *7* (9), 26-35.
13. Q-S, A.; Bobermin, L. D.; Tramontina, A. C.; Wartchow, K. M.; Tagliari, B.; Souza, D. O.; Wyse, A. T. S.; Goncalves, C. A. Oxidative stress mediated by NMDA, AMPA/KA channels in acute hippocampal slices: Neuroprotective effect of resveratrol, *Toxicol. in Vitro.* **2014**, *28*, 544-551.
14. U-P, I.; Calvo, M. I. Flavonoids as acetylcholinesterase inhibitors, *Curr. Med. Chem.* **2011**, *18*, 5289-5302.
15. J, H. F.; Zhang, H.Y. Theoretical evaluation of flavonoids as multipotent agents to combat Alzheimer's disease. *J. Mol. Struc-Theochem.*, **2006,** *767*, 3-9.
16. (a) da Silva, B. P.; Bernardo, R. R.; Parente, J. P.; Flavonol glycosides from Costusspicatus, *Phytochemistry*, **2000**, *53*, 87-92. (b) Vilegas, W.; Sanommiya, M.; Rastrelli, L.; Pizza, C., Isolation and structure elucidation of two new flavonoid glycosides from the infusion of *Maytenusaquifolium* leaves. Evaluation of the antiulcer activity of the infusion, *J. Agric. Food Chem.*, **1999**, *47*, 403-406. (c) Li, Z.; Ngojeh, G.; Witt, P. D.; Zheng, Z.; Chen, M.; Lainhart, B.; Li, V.; Felpo, P. Synthesis of a library of glycosylated flavonols, *Tetrahedron Lett.* **2008**, *49*, 7243-7245.
17. (a) Mughal, E. U.; Ayaz, M.; Hussain, Z.; Hasan, A.; Sadiq, A.; Riaz, M.; Malik, A.; Hussain, S.; Choudhary, M. I. Synthesis and antibacterial activity of substituted flavones,4-thioflavones and 4-iminoflavones, *Bioorg. Med. Chem.* **2006**, *14*, 4704-

4711. (b) Mughal, E. U.; Sadiq, A.; Khan, B. A.; Zafar, M. N.; Ahmed, I.; Zubair, M. Synthesis, molecular docking studies and biological evaluation of 3-iminoaurones as acetylcholinesterase and butyrylcholinesterase inhibitors, *Letters in Drug Design and Discovery*, **2017**, *14*, 1035-1041.

18. Mughal, E. U.; Sadiq, A.; Murtaza, S.; Rafique, H.; Zafar, M. N.; Riaz, T.; Khan, B. A.; Hameed, A.; Khan, K. M. Synthesis, structure-activityrelationship and moleculardocking of 3-oxoaurones and 3-thioaurones as acetylcholinestrase and butyrylcholinestreaseinhibitors. *Bioorg. Med. Chem.* **2017**, *25*, 100-106, and references quoted therein.

19. Sousa, J. L. C.; Proença, C.; Freitas, M.; Fernandes, E.; Silva, A. M. S.; New polyhydroxylated flavon-3-ols and 3-hydroxy-2-styrylchromones: synthesis and ROS/RNS scavenging activities, *Eur. J. Med. Chem.* **2016**, *119*, 250-259, and references quoted therein.

Graphical Abstract

Synthesis, Structure-Activity Relationship and Molecular Docking Studies of 3-*O*-Flavonol Glycosides as Cholinesterase Inhibitors

Ehsan Ullah Mughal*, Asif Javid, Amina Sadiq, Shahzad Murtaza, Muhammad Naveed Zafar, Bilal Ahmad Khan, Sajjad Hussain Sumra, Muhammad Nawaz Tahir, Kanwal, Khalid Mohammed Khan